

# Polysiloxane–poly(fluorinated acrylate) interpenetrating polymer networks: Synthesis and characterization

Vincent Darras<sup>a</sup>, Odile Fichet<sup>a</sup>, Françoise Perrot<sup>a</sup>, Sylvie Boileau<sup>b</sup>, Dominique Teyssié<sup>a,\*</sup>

<sup>a</sup> *Laboratoire de Physicochimie des Polymères et des Interfaces (LPPI), Université de Cergy-Pontoise – 5, mail Gay-Lussac, Neuville-sur-Oise, 95031 Cergy-Pontoise Cedex, France*

<sup>b</sup> *Laboratoire de Recherche sur les Polymères, UMR 7581 CNRS, 2, rue H. Dunant, 94320 Thiais, France*

Received 21 July 2006; received in revised form 27 November 2006; accepted 28 November 2006

Available online 8 January 2007

## Abstract

Combinations of fluorinated and silicone based elastomers were elaborated through the *in situ* synthesis of interpenetrating polymer networks (IPNs). The PDMS network was formed by dibutyltin dilaurate catalyzed addition between the hydroxy end groups of  $\alpha,\omega$ -(3-hydroxypropyl)-polydimethylsiloxane (PDMS) and a pluriisocyanate cross-linker. The poly(fluorinated acrylate) (polyAcRf6) network was obtained from free-radical copolymerization of a fluorinated acrylate with ethylene glycol dimethacrylate in the presence of dicyclohexyl peroxydicarbonate as the initiator. IPNs with different relative weight proportions of the fluorinated vs silicone partners were characterized by DMTA and DSC. Density refractive index and contact angle measurements reveal a satisfactory interpenetration degree of PDMS and polyAcRf6 networks. In addition, these materials present an unusual variation of density values and of the surface properties as a function of the relative weight composition. © 2006 Elsevier Ltd. All rights reserved.

**Keywords:** Polydimethylsiloxane; Fluorinated acrylate; Interpenetrating polymer network

## 1. Introduction

Various strategies have been developed in order to design fluorine-containing elastomers maintaining rubber-like elasticity in extremely severe environments including exposure to high temperatures and corrosive chemicals. The synthesis of fluorinated compounds leading to elastomers showing high solvent resistance, thermal stability, low-temperature flexibility and high fluorine content presents some internal conflicts because of the repulsions between the hydrocarbon and fluorocarbon groups which are necessarily associated in the same molecule. In addition, these compounds generally are liquid or waxy solids above 0 °C. In order to prevent permanent flow deformation under an imposed strain, these flexible macromolecules must be cross-linked.

Fluorinated polysiloxane single networks have been prepared by sol–gel reaction of fluorinated polysiloxanes bearing terminal trialkoxysilane moieties with silanol cross-linkers [1], or fluorinated polysiloxanes bearing silanol end groups with (tridecafluoro-1,1,2,2-tetrahydrooctyl)-triethoxysilane [2]. Similar single networks were also synthesized by hydrosilylation reaction of tetravinyltetramethylcyclotetrasiloxane ( $D_4^{Vi}$ ) [3], divinyltetramethyldisiloxane [4] or fluorinated divinyl telechelic polysiloxane [5] with polysiloxanes containing fluorinated side chains and Si–H groups. For example, Fuduka et al. [6] have synthesized networks starting from perfluorinated vinyl ether end chains which react on Si–H terminated polysiloxanes bearing  $-\text{CH}_2-\text{CH}_2-\text{C}_8\text{F}_{17}$  side-groups. Those fluorinated polysiloxane networks are mainly used as protecting coatings. However, the synthesis pathways leading to the telechelic precursors of those networks do not allow a fine tuning of the molar mass and polymolecularity, as well as of their functionality which should be as close as possible to two. In addition, fluorinated polysiloxane networks do not show convenient

\* Corresponding author. Tel.: +33 1 34 25 70 50; fax: +33 1 34 25 70 70.  
E-mail address: [dominique.teyssie@chim.u-cergy.fr](mailto:dominique.teyssie@chim.u-cergy.fr) (D. Teyssié).

mechanical properties at room temperature which restrains the development of these materials in new applications.

An adequate solution, which could lead to the elaboration of materials endowed with the desirable characteristics of fluorinated polysiloxane networks without showing their drawbacks, is to combine two independent polymers showing polysiloxane properties on one hand, and fluorinated ones on the other hand, into an interpenetrating polymer network (IPN) architecture. The aim of the elaboration of such types of polymer associations in general is to obtain materials with better mechanical properties, an increased resistance to degradation and a potential synergy of the properties of their components.

IPNs are defined as combinations of two or more polymer networks synthesized in juxtaposition [7,8]. The entanglement of two cross-linked polymers leads to forced miscibility compared with usual incompatible blends, and the resulting materials exhibit a good dimensional stability. IPNs can be prepared through an *in situ* synthesis where all reactants are mixed together. According to this strategy, the syntheses of the two networks are started at the same time leading either to their simultaneous or sequential formation. Hence, the reaction mechanisms leading to the formation of the two network partners must be of different nature, otherwise a single copolymer network (bicomponent network or co-network) is formed through crossed reactions.

In the present work, the synthetic pathway for preparing IPNs composed of polydimethylsiloxane (PDMS) and a poly-(fluorinated acrylate) (polyAcRf6) is described. The synthesis involves an *in situ* process where the two networks are then formed more or less simultaneously as it will be shown. The conversions as a function of time of the reactive functions involved in the synthesis of each network during the IPN formation have been investigated by near FTIR spectroscopy. In order to examine the extent of network interpenetration, thermomechanical properties, density and refractive index of the resulting materials have been studied as a function of PDMS/polyAcRf6 composition. Finally the surface properties of those IPNs have been characterized by contact angle measurements.

## 2. Experimental section

### 2.1. Materials

3,3,4,4,5,5,6,6,7,7,8,8,8-Tridecafluoro-1-octanol (Aldrich), dibutyltindilaurate (DBTDL, Aldrich), ethylene glycol dimethacrylate (EGDMA, Aldrich), acryloyl chloride (Acros) and Desmodur<sup>®</sup> N3300 (Bayer) (NCO content:  $21.8 \pm 0.3$  wt% according to the supplier) are used as received. This last compound is described as an isocyanurate mixture resulting from the condensation of three to several hexamethylene diisocyanate molecules and mainly composed of mono-, di- and tri-isocyanurates with a global functionality higher than 2 [9]. Thus mere “tris(6-isocyanatohexyl)isocyanurate” is not a proper description and the compound is referred to as the cross-linking agent. Dicyclohexylperoxydicarbonate (DCPD, Groupe Arnaud) is dried under vacuum before use. Toluene (Carlo Erba, puro) and dichloromethane ( $\text{CH}_2\text{Cl}_2$ , Carlo Erba) are distilled and

dried before use. 1,1,2-Trichloro-2,2,1-trifluoroethane (F113) and  $\alpha,\omega$ -(3-hydroxypropyl)poly(dimethylsiloxane) (PDMS oligomer) are kindly provided by Atochem and Rhodia, respectively. PDMS oligomer ( $M_{n,SEC} = 1140 \text{ g mol}^{-1}$ ,  $I_p = 2$  in THF,  $M_{n,NMR} = 1100 \text{ g mol}^{-1}$  in  $\text{CDCl}_3$ ) is dried under vacuum before use.

### 2.2. Material synthesis

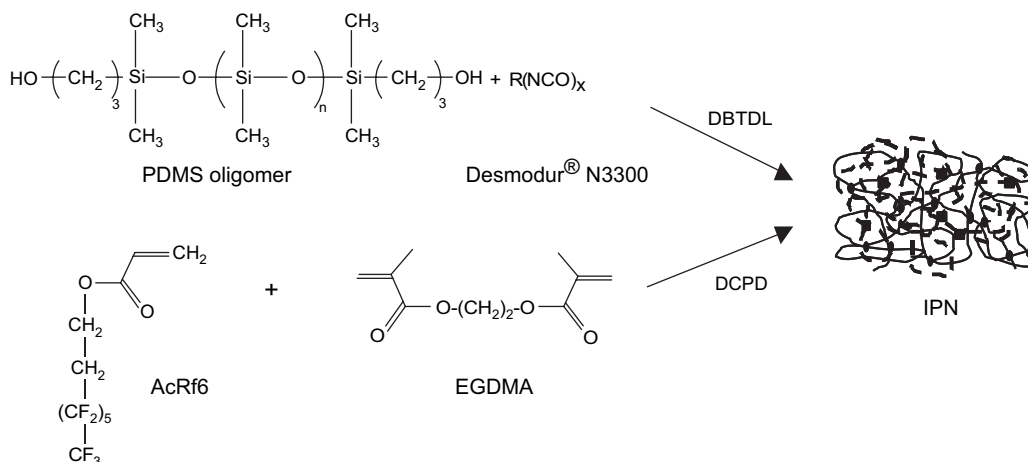
$\alpha,\omega$ -(3-Hydroxypropyl)poly(dimethylsiloxane) (1 g,  $1.75 \times 10^{-3}$  OH mol) and Desmodur<sup>®</sup> N3300 (0.40 g,  $2.11 \times 10^{-3}$  NCO mol,  $[\text{NCO}]/[\text{OH}] = 1.2$ ) are dissolved in 2 mL toluene to which the catalyst DBTDL (16 mg,  $2.53 \times 10^{-5}$  mol,  $[\text{DBTDL}]/[\text{OH}] = 0.014$ ) is added. The mixture is poured under argon into a mould made from two glass plates clamped together and sealed with a 1 mm thick Teflon<sup>®</sup> gasket. The mould is heated in an oven at  $55^\circ\text{C}$  for 15 h. After release from the mould, a transparent film is obtained after taking off toluene under vacuum.

The fluorinated acrylate (AcRf6) is synthesized as follows: 7.28 g of 3,3,4,4,5,5,6,6,7,7,8,8,8-tridecafluoro-1-octanol (0.02 mol), 2.43 g triethylamine (0.024 mol) and 100 mL  $\text{CH}_2\text{Cl}_2$  are placed in a three-neck flask fitted with a condenser. Acryloyl chloride (1.79 mL, 0.022 mol) is added dropwise at  $0^\circ\text{C}$ . Then, the mixture is stirred at  $40^\circ\text{C}$  for 6 h. At the end of the reaction, the mixture is washed several times with a sodium hydroxide solution to neutral pH. The crude product is dried on  $\text{MgSO}_4$ . After filtration, the solvent is eliminated under vacuum. The obtained product, 3,3,4,4,5,5,6,6,7,7,8,8,8-tridecafluorooctyl acrylate (PolyAcRf6) is purified on a silica column with  $\text{CH}_2\text{Cl}_2$  as the eluent and characterized by  $^1\text{H}$  NMR ( $\text{CDCl}_3$ ).

A single fluorinated network is prepared as follows: AcRf6 (1 g,  $2.4 \times 10^{-3}$  mol), EGDMA (24 mg,  $1.2 \times 10^{-4}$  mol,  $[\text{EGDMA}]/[\text{AcRf6}] = 0.05$ ) and DCPD (3.8 mg,  $1.3 \times 10^{-4}$  mol,  $[\text{DCPD}]/[\text{C}=\text{C}] = 0.05$ ) are mixed under argon for 30 min. The mixture is poured into a mould made from two glass plates clamped together and sealed with a 1 mm thick Teflon<sup>®</sup> gasket. The mould is heated in an oven at  $55^\circ\text{C}$  for 15 h and a transparent film is obtained. The synthesis of this single network does not require a solvent.

A PDMS/polyAcRf6 (50/50) IPN is synthesized as follows (Scheme 1):  $\alpha,\omega$ -(3-hydroxypropyl)poly(dimethylsiloxane) (PDMS oligomer, 1 g,  $1.75 \times 10^{-3}$  OH mol) is dissolved in 2 mL toluene under argon together with 0.40 g Desmodur<sup>®</sup> N3300 ( $2.11 \times 10^{-3}$  NCO mol,  $[\text{NCO}]/[\text{OH}] = 1.2$ ), 1 g AcRf6 ( $2.4 \times 10^{-3}$  mol), 24 mg EGDMA ( $1.2 \times 10^{-4}$  mol,  $[\text{EGDMA}]/[\text{AcRf6}] = 0.05$ ) and 3.8 mg DCPD ( $1.3 \times 10^{-4}$  mol,  $[\text{DCPD}]/[\text{C}=\text{C}] = 0.05$ ). Then, 16 mg DBTDL ( $2.53 \times 10^{-5}$  mol,  $[\text{DBTDL}]/[\text{OH}] = 0.014$ ) is added just before introducing the mixture into a mould as described previously. The mould is heated in an oven at  $55^\circ\text{C}$  for 15 h and toluene is then taken off under vacuum.

IPNs with polyAcRf6 contents ranging from 25 to 75% by weight are synthesized keeping the same proportions among monomer, cross-linker and catalyst or initiator as described for the synthesis of each single network. All investigated



Scheme 1. Synthesis pathway of PDMS/polyAcRf6 IPNs.

PDMS/polyAcRf6 compositions are reported in weight by weight ratio. Thus, an IPN obtained from a mixture of 0.75 g  $\alpha,\omega$ -(3-hydroxypropyl)poly(dimethylsiloxane) and 0.25 g AcRf6 will be noted as a PDMS/polyAcRf6 (75/25) IPN.

### 2.3. Analytical techniques

The polymerization kinetics can be followed in the bulk and in real time in the near and middle infrared (NIR and MIR) regions ( $7500\text{--}1800\text{ cm}^{-1}$ ). The polyAcRf6 network formation is followed by monitoring the disappearance of the H–C bonds of the H–C=CH<sub>2</sub> group of the acrylate monomer at  $6175\text{ cm}^{-1}$ . Similarly, the PDMS network formation is followed by quantifying the disappearance of the isocyanate band at  $2270\text{ cm}^{-1}$ . It was first checked that all reaction mixtures obey the Beer–Lambert law in the concentration and temperature ranges used in this work. Indeed, for each absorption band, the area is directly proportional to the monomer concentration, thus the conversion–time profile can be easily derived from the spectra recorded as a function of time. The conversion of reactive bonds can be calculated as  $p = 1 - (A_t/A_0)$  from the absorbance values where the symbols have the usual meaning and the subscripts 0 and  $t$  denote reaction times.

IPNs are directly synthesized in a disposable home-made IR cell. Glass windows and 3 mm thick gaskets are used to record the acrylate conversion because the corresponding absorption band is located in the near infrared. On the other hand, CaF<sub>2</sub> fluorine windows and 250  $\mu\text{m}$  thick gaskets are used when the NCO conversion is recorded in the middle infrared region. The IR cell is inserted in an electrical heating jacket with an automatic temperature controller (Graseby Specac). The temperature of the cell holder is constant within  $\pm 1\text{ }^\circ\text{C}$  of the set temperature. The infrared spectra are recorded with a Bruker spectrometer (Equinox 55) in the range  $7000\text{--}1800\text{ cm}^{-1}$  by averaging 10 consecutive scans with a resolution of  $4\text{ cm}^{-1}$ . Scan accumulations are repeated every 2 min during the kinetic measurements in order to establish a full time–conversion curve.

In order to determine the amount of unreacted starting materials in the final products and thus the extent of covalent bond formation in the networks, single networks and IPNs are extracted in a Soxhlet extractor with F113 for 48 h, AcRf6, polyAcRf6 [10] and PDMS oligomer being soluble in this solvent. After extraction, the sample is dried under vacuum and then weighed. The extracted content (EC) is given as a weight percentage:

$$\text{EC} (\%) = \frac{(W_0 - W_E)}{W_0} \times 100$$

where  $W_0$  and  $W_E$  are the weights of samples before and after extraction, respectively.

Dynamic mechanical thermal analysis (DMTA) measurements are carried out on film samples with a Q800 apparatus (TA Instruments) operating in tension mode. Experiments are performed at a 1 Hz frequency and a heating rate of  $3\text{ }^\circ\text{C min}^{-1}$  from  $-120$  to  $100\text{ }^\circ\text{C}$  after stabilization at  $-140\text{ }^\circ\text{C}$  for 5 min. Typical dimensions of the samples are  $7\text{ mm} \times 8\text{ mm} \times 0.8\text{ mm}$ . The set up provides the storage and loss moduli ( $E'$  and  $E''$ ) and the damping parameter or loss factor ( $\tan \delta$ ). All storage modulus values are normalized at 2000 MPa at  $-120\text{ }^\circ\text{C}$  when the materials are in a glassy state, in order to compare their relative evolution with increasing temperature.

DSC measurements are carried out on a DSC Q100 (TA Instruments) apparatus with a heating rate of  $20\text{ }^\circ\text{C min}^{-1}$  from  $-80$  to  $150\text{ }^\circ\text{C}$ .

Refractive index measurements are made at the wavelength of the sodium D ray ( $\lambda_0 = 589\text{ nm}$ ) using a Prolabo refractometer with a thermoregulation at  $25\text{ }^\circ\text{C}$ . The densities are measured at  $25\text{ }^\circ\text{C}$ , using an Accupyc 1330 (Micromeritics) picnometer. The final given value is averaged from 25 measurements carried out for each sample. The standard deviation on the mean density value is  $0.002\text{ g/cm}^3$ . The measured densities and refractive indices are compared to the values calculated from the Lorentz–Lorentz equation [11]. The relationship between the molar refraction,  $R$ , the density,  $\rho$ , and the refractive index,  $n$ , is given by

$$R = \frac{n^2 - 1}{n^2 + 2} \times \frac{M}{\rho} \quad (1)$$

where  $M$  is the molar mass of the polymer. The specific refraction of a polymer is defined as

$$R' = \frac{R}{M} = \frac{1}{d} \times \frac{n^2 - 1}{n^2 + 2}$$

where  $d$  is the polymer density.

For a combination of two networks, the specific refraction,  $R'$  is given by

$$R' = x_1 R'_1 + x_2 R'_2 \quad (2)$$

where  $x_1$  and  $x_2$  are the volume fractions of networks 1 and 2, respectively.  $R'_1$  and  $R'_2$  are the specific refractions of each network and can be calculated from the refractive indices ( $n_1$  and  $n_2$ ) and the densities ( $d_1$  and  $d_2$ ) measured on the single networks. Thus  $R'$  can be calculated for each IPN composition. From  $R'$  and density, the refractive index of the IPNs can be calculated using Eq. (1).

The liquid-film contact angle ( $\theta$ ) is determined from image recordings by video microscope after deposition of a 25  $\mu$ L water drop at 20 °C on the single network and IPN surfaces. The values of equilibrium contact angles are computed after processing the images with a frame grabbing software (Drope Shape Analysis). All equilibrium angles  $\theta$  represent a mean value for 6–8 drops applied on different spots of the material surface. The experimental error is about 2%.

### 3. Results and discussion

Single PDMS and fluorinated polyacrylate networks have been synthesized and characterized before combining them in an IPN architecture.

#### 3.1. Single networks

The single fluorinated acrylate (polyAcRf6) network is formed by free-radical copolymerization of a perfluoroalkyl-acrylate with EGDMA ([EGDMA]/[AcRf6] = 0.05) as the cross-linker in the bulk. The single polyAcRf6 network synthesis is initiated with DCPD ([DCPD]/[C=C] = 0.05) at 55 °C. This particular temperature leads to a fast network formation, which is imperative for obtaining a correctly interpenetrating material as will be shown later on. The obtained transparent single polyAcRf6 network is subjected to an F113 extraction for 48 h. The extracted product amount is 1 wt%, indicating a near completion of the polyAcRf6 cross-linking process.  $^1\text{H}$  NMR analysis shows that the soluble fraction is essentially composed of linear polyAcRf6 without residual AcRf6 monomer.

The storage modulus ( $E'$ ) and the loss tangent ( $\tan \delta$ ) of the single polyAcRf6 network are reported in Fig. 1a. Three temperature domains are observed. From  $-120$  to  $-10$  °C, the storage modulus  $E'$  is almost constant at 2000 MPa: the polymer is in its glassy state and the response of the network is

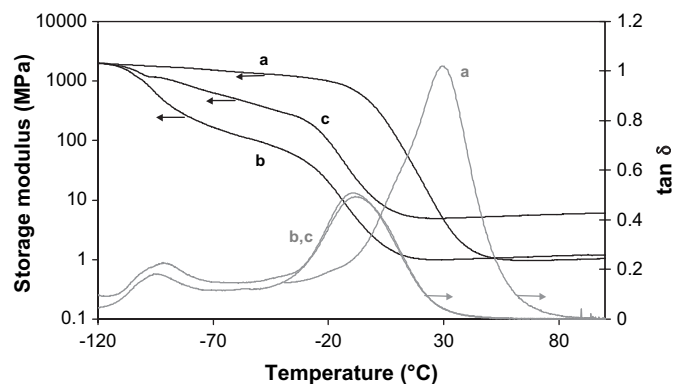


Fig. 1. Storage modulus and  $\tan \delta$  vs temperature. PolyAcRf6 single network (a) and PDMS single network before (b) and after (c) Soxhlet extraction with F113 for 48 h.

mainly elastic. Above  $-10$  °C, a strong decay of the elastic part of the modulus  $E'$  is observed while  $\tan \delta$  vs temperature curve presents a maximum at  $+30$  °C ( $\tan \delta = 1.0$ ). The elastic part of the modulus  $E'$  reaches a plateau (rubbery modulus) at 1 MPa at temperatures higher than 45 °C.

The PDMS single network is synthesized *via* a dibutyltin-dilaurate (DBTDL) catalyzed alcohol/isocyanate condensation reaction leading to urethane bonds cross-linked between  $\alpha,\omega$ -(3-hydroxypropyl)poly(dimethylsiloxane) and the pluriisocyanate. Due to the immiscibility of the PDMS oligomer and the pluriisocyanate, it appears unavoidable to add a significant amount of toluene (2 mL per gram of PDMS). The reaction mixture is then heated at 55 °C for 15 h. After evaporation of the residual toluene under vacuum an insoluble transparent material containing a low amount of extracted products (4 wt%) as found by a Soxhlet extraction with F113 is obtained. It was checked that F113 correctly swells the PDMS single network (maximum swelling ratio: 200 wt%) and can thus be considered as a suitable extraction solvent for the PDMS oligomers.  $^1\text{H}$  NMR analysis shows that the soluble fraction is essentially composed of PDMS oligomer and traces of isocyanate cross-linker.

Only one glass transition ( $T_g$ ) is detected at  $-25$  °C by DSC for this single PDMS network, a value which is much higher than the  $T_g$  of linear PDMS ( $T_g = -123$  °C) [12]. This rather high  $T_g$  value should be due to physical interactions between urethane groups. Indeed, Clarson et al. [13] have shown that the  $T_g$  of a given PDMS network mainly depends on the cross-linker's chemical nature and much less on the length of the PDMS chains between two cross-links.

Thermomechanical properties of this single PDMS network are reported in Fig. 1b. Below  $-120$  °C, the storage modulus is almost constant at 2000 MPa. Above  $-120$  °C, it decreases rapidly and reaches a plateau value at about 200 MPa. Then a second modulus decrease is observed from 100 to 2 MPa between  $-25$  and  $+10$  °C. Above 10 °C, the rubbery plateau remains steady at 2 MPa. Both the decreases of  $E'$  are associated to a  $\tan \delta$  peak at  $-94$  and  $-8$  °C, respectively. The peak at  $-94$  °C could be associated hypothetically to the mechanical relaxation of uncross-linked PDMS chains. In order to check this point, a DMTA curve is recorded on a PDMS

network extracted sample (Fig. 1c). The storage modulus of the sample is now 10 times higher than that of the non-extracted sample. However, the peak at  $-94\text{ }^{\circ}\text{C}$  is still detected. Thus, it could be assigned rather to the presence of monofunctional PDMS chains acting as plasticizing agents. Indeed, MALDI-TOF analysis shows that the PDMS precursor contains monofunctional chains and different  $D_n$  cycles. The mechanical relaxation at  $-94\text{ }^{\circ}\text{C}$  will not be further commented in this study. On the other hand, the  $\tan \delta$  peak at  $-8\text{ }^{\circ}\text{C}$  is unaffected by the extraction step. It can thus be associated with the mechanical relaxation of a single PDMS network, in coherence with the  $-25\text{ }^{\circ}\text{C}$   $T_g$  value measured by DSC.

### 3.2. Interpenetrating polymer networks

All IPNs have been synthesized according to an *in situ* strategy, i.e. all reagents for the formation of both single networks are mixed together: monomers, cross-linkers, initiator and catalyst form a clear solution in toluene (2 mL per gram of reaction mixture). The whole synthesis is carried out at  $55\text{ }^{\circ}\text{C}$  for 15 h.

The formation rates of silicone and fluorinated networks in the PDMS/polyAcRf6 (50/50) IPNs are monitored by FTIR spectroscopy (Fig. 2). The fluorinated and PDMS network formations are followed by monitoring the disappearance of the absorption band of the vinyl C–H bonds of the acrylate group in the monomer at  $6175\text{ cm}^{-1}$  [14] and of the NCO bond at  $2270\text{ cm}^{-1}$  [15] yielding the corresponding function conversion vs time curves.

Kinetic FTIR studies of the formation of PDMS/polyAcRf6 (50/50) IPNs were performed on a series of starting mixtures where the nature and the amount of initiator (AIBN, DCPD) as well as the temperature were changed. It was shown that transparent materials could be obtained only with DCPD as the initiator and only when the temperature is equal to  $55\text{ }^{\circ}\text{C}$ . In these conditions it clearly appears that the PolyAcRf6 network forms first (Fig. 2).

As expected, the AcRf6 polymerization is very fast since the maximum conversion is reached after 8 min at  $55\text{ }^{\circ}\text{C}$ . This result is in agreement with the decomposition constant value of DCPD at  $55\text{ }^{\circ}\text{C}$  ( $k_d = 6 \times 10^{-3}\text{ min}^{-1}$  [16]). The NCO conversion increases at the same rate as that of the fluorinated

acrylate up to 0.20 conversion. Then this last rate slows down but keeps a steady slope and the PDMS network formation is achieved after about 60 min at  $55\text{ }^{\circ}\text{C}$ . The inflexion in the conversion–time curve for the NCO group corresponds exactly with the time when the fluorinated network formation undergoes a Trommsdorff effect, with a remarkable increase in the network rate of formation. Thus, although the polyAcRf6 network is in a rubbery state at the synthesis temperature, it seems that a steric hindrance corresponding to the rapid formation of a tight AcRf6 mesh will slow down the PDMS oligomers' mobility and thus interfere with network formation.

Those experimental conditions lead to transparent materials as far as the following weight proportions are concerned: PDMS/polyAcRf6 (75/25) and (50/50) IPNs. However, whatever the experimental conditions (nature and amount of initiator and synthesis temperature), the PDMS/polyAcRf6 (25/75) IPN could never be obtained in a transparent state.

In order to ensure completion of the cross-linking reactions, all IPN samples are cured for 15 h at  $55\text{ }^{\circ}\text{C}$ . Indeed, post-curing at a higher temperature than  $55\text{ }^{\circ}\text{C}$  is difficult in the presence of toluene without bubble evolution. Under those experimental conditions, whatever the IPN composition, the extracted material amounts are lower than 8 wt% and their analysis by  $^1\text{H}$  NMR shows that they are mainly composed of linear polyAcRf6.

DSC measurements carried out on three composition IPNs show one glass transition only, the position of which depends on the IPN composition (Table 1). PDMS/polyAcRf6 (75/25), (50/50) and (25/75) show a  $T_g$  at  $-20$ ,  $-14$  and  $-8\text{ }^{\circ}\text{C}$ , respectively. The fact that the  $T_g$  values of the two single networks are close to each other ( $T_g$  (PDMS) =  $-25\text{ }^{\circ}\text{C}$  and  $T_g$  (polyAcRf6) =  $+3\text{ }^{\circ}\text{C}$ ) can explain why only one broad transition is observed in the different IPNs.

The interpenetration degree of both networks into the IPN architecture can be approached by dynamic mechanical thermal analysis (DMTA) which is often a sensitive technique to detect the occurrence of phase separation. Generally, the domain size is considered of the order of 5–50 nm if only one mechanical relaxation is detected in the loss factor ( $\tan \delta$ )–temperature curve. This single relaxation corresponding to an interpenetrating phase is located at a temperature between those of the single networks [17]. Thus, in order to characterize the interpenetration degree of PDMS and polyAcRf6 networks in the IPN architecture, DMTA measurements are carried out on the PDMS/polyAcRf6 (75/25), (50/50) and (25/75) IPNs (Fig. 3). All storage moduli are normalized at 2000 MPa at  $-120\text{ }^{\circ}\text{C}$  in order to analyze the modulus evolution as a function of the AcRf6 weight proportion in the IPN.

Table 1

Glass transition temperature ( $T_g$ ) measured by DSC and mechanical relaxation temperature ( $T_\alpha$ ) measured by DMTA for different single networks and PDMS/polyAcRf6 IPNs

PDMS/polyAcRf6 composition	100/0	75/25	50/50	25/75	0/100
$T_g$ ( $^{\circ}\text{C}$ )	$-25$	$-20$	$-14$	$-8$	$+3$
$T_\alpha$ ( $^{\circ}\text{C}$ )	$-8$	$-5$	$0$	$0/+25$	$+30$

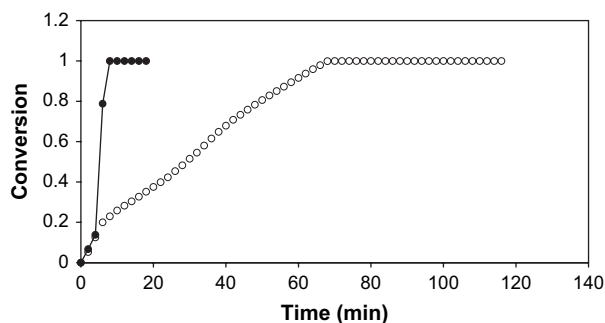


Fig. 2. (●) Acrylate and (○) NCO groups' time–conversion plot for a PDMS/polyAcRf6 (50/50) reaction mixture.  $[\text{EGDMA}]/[\text{AcRf6}] = 0.05$ .  $[\text{DCPD}]/[\text{C}=\text{C}] = 0.05$ .  $[\text{NCO}]/[\text{OH}] = 1.2$ .  $[\text{DBTDL}]/[\text{OH}] = 0.014$ .  $T = 55\text{ }^{\circ}\text{C}$ .

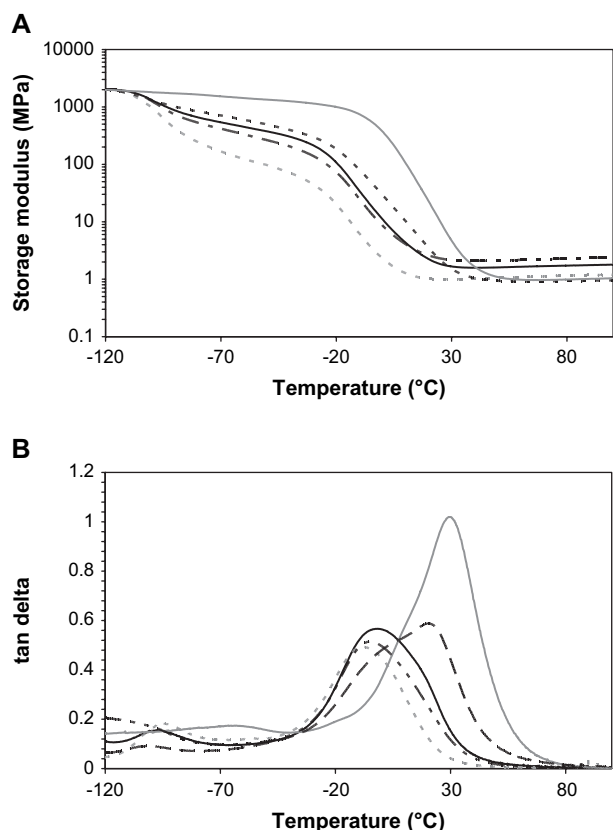


Fig. 3. Storage modulus (A) and  $\tan \delta$  (B) of PDMS/polyAcRf6 (75/25) (— —), (50/50) (—) and (25/75) (— —) IPNs vs temperature plots. PDMS (---) and polyAcRf6 (—) single network values are reported for comparison.

All storage modulus vs temperature curves show the same shape whatever the IPN composition. A small decrease at  $-110^\circ\text{C}$  is explained by the presence of the monofunctional chains in the PDMS network. When the temperature increases, the storage modulus decreases rapidly at a temperature depending on the IPN composition. Above  $+35^\circ\text{C}$ , the storage modulus hardly depends on the AcRf6 content. Those materials do not flow at high temperatures and a constant modulus value of around  $0.8\text{ MPa}$  is observed up to  $150^\circ\text{C}$  (rubbery plateau).

On the other hand, the  $\tan \delta$ –temperature curve of PDMS/polyAcRf6 (25/75) IPNs does not show a single peak (Fig. 3b). Instead, the bimodal peak extends from about  $-50^\circ\text{C}$  to  $+50^\circ\text{C}$  with a maximum  $\tan \delta = 0.6$  at  $+25^\circ\text{C}$  and a shoulder at  $0^\circ\text{C}$ . These two peaks are characteristic of a rich polyAcRf6 phase and a rich PDMS phase, respectively. Considering the  $\tan \delta$  maximum position for the single networks ( $T_\alpha(\text{PDMS}) = -8^\circ\text{C}$  and  $T_\alpha(\text{polyAcRf6}) = +30^\circ\text{C}$  – Table 1), the mechanical relaxation temperatures of the two partner networks in this IPN are somewhat shifted one towards the other. This is indicative of weak but existing interactions between the networks in the material although their interpenetration cannot be qualified as satisfactory. This result is in agreement with the macroscopic aspect of the IPN, which is translucent.

As far as PDMS/polyAcRf6 (75/25) and (50/50) IPNs are concerned, only one broad mechanical relaxation is observed,

the  $\tan \delta$  peak lying at an intermediate temperature between those of the two single networks. This behaviour is characteristic of a material in which both networks are correctly interpenetrating. The  $\alpha$  relaxation temperature increases hardly from  $-5$  to  $0^\circ\text{C}$  when the AcRf6 amount in the IPN increases from 25 to 50 wt%. However, it is difficult to derive precise information in this case because of the proximity of the mechanical relaxation temperatures of the two single networks ( $T_\alpha(\text{PDMS}) = -8^\circ\text{C}$  and  $T_\alpha(\text{polyAcRf6}) = +30^\circ\text{C}$  – Table 1). For this reason, other techniques have been used in order to obtain more information about the interpenetration degree of the two partner networks.

Indeed the specific volume of a material varies linearly with the weight composition in the case of non-miscible polymer blends in which no adhesion and no molecular mixing occur at the phase boundary [18]. It is thus interesting to compare linear variation with the specific volume of the IPN in order to get an estimation of their interpenetration degree.

Single PDMS and polyAcRf6 networks show a density of  $1.073$  and  $1.732 \pm 0.001$ , respectively, which is in agreement with the values reported in the literature for silicone and fluorinated compounds, respectively [12]. Those values correspond with specific volumes equal to  $0.932$  and  $0.577 \pm 0.001\text{ g cm}^{-3}$  for PDMS and polyAcRf6 single networks, respectively. Fig. 4 shows the specific volumes calculated from the single network and IPN measured densities as a function of the material weight composition. Thus, for all IPN compositions the specific volumes are higher than the values of the linear combination of those of the single networks and this behaviour cannot be matched with that of a blend in which polymers are not miscible. The PDMS/polyAcRf6 (50/50) IPN exhibits a specific volume deviation corresponding to a 3% relative density variation with respect to typical blend behaviour. Similar volume expansions have also been observed in IPN architectures such as polydimethylsiloxane/bis(diethylene glycol allyl carbonate) [19], epoxy DGEBA/methacrylate DGEBA [20] and hydrogenated castor oil based uralkyd resin/poly(butylmethacrylate) [21] which present volume expansions equal to 4, 2 and 10%, respectively. In other words, PDMS/polyAcRf6 IPNs possess densities lower than those predicted by additive volume law that suggests the presence

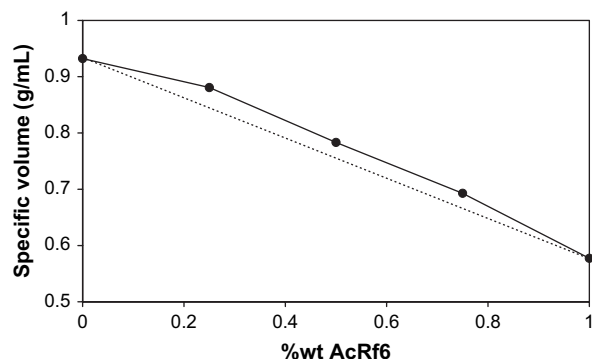


Fig. 4. Specific volume of PDMS/polyAcRf6 IPNs vs AcRf6 weight proportion (●) from density measurements and (dotted line) calculated by additive law of the single network specific volumes.

of repulsion forces between partner networks. This is in agreement with the known incompatibility of fluorinated compounds with non-fluorinated ones. However, those repulsions have been overcome by the counteracting cross-linking effect since no macroscopic phase separation is observed. Indeed, the PDMS/polyAcRf6 (50/50) and (75/25) IPNs are transparent. The results of the density measurement support the conclusion from DMTA analysis: PDMS and polyAcRf6 networks do exhibit some interaction within the IPNs.

The interpenetration extent of the individual networks within an IPN architecture can also be derived from the optical aspect of the material. Indeed, the IPN transparency is somewhat related to phase separation: the more transparent the material, the lesser the phase separation [8]. However, this is true only if the difference between the refractive indices of the single networks is significant ( $\Delta n > 0.02$ ). Single PDMS and polyAcRf6 network refractive index measurements lead to 1.443 and 1.363, respectively at 25 °C and these values compare with those reported in the literature (1.43 and 1.37 for PDMS and fluorinated polyacrylates, respectively) [12]. The difference ( $\Delta n = 0.06$ ) is sufficiently important to yield an opaque material, should a significant phase separation occur during the IPN synthesis.

PDMS/polyAcRf6 (75/25) and (50/50) IPNs are transparent, indicating the absence of such a significant phase separation. On the other hand, the PDMS/polyAcRf6 (25/75) IPN is translucent, meaning that some phase separation occurs for this composition. The result is in agreement with DMTA measurements, which show both a peak (corresponding to polyAcRf6 rich phase) and a shoulder (corresponding to PDMS rich phase) for this last composition.

The PDMS/polyAcRf6 IPN refractive indices measured for various compositions at 25 °C are reported in Fig. 5. As expected from the values of the individual network indices, decreasing the polyAcRf6 network proportion in the IPN architecture leads to an increase of the refractive index of the final material. Indices vary from 1.406 to 1.436 when the AcRf6 volume fraction decreases from 0.65 to 0.17 (from 75 to 25 wt%). Thus, it is possible to prepare materials with a variable refractive index by playing with the AcRf6 proportion. On the

other hand, the cross-linking density of the polyAcRf6 network does not affect the values of the refractive indices (results not shown) [22].

The refractive indices values can be calculated from single network indices according to the Lorentz–Lorentz equation [11] (see Section 2).

First, the experimental IPN density is used for the calculation of the IPN refractive index. The measured and calculated values of the indices are in perfect agreement (Fig. 5). Second, those indices have been again calculated using the density derived from an additive law of the single network densities. In this case, the calculated indices are significantly higher than the experimental ones. Thus, the interaction between both networks within this IPN architecture leads to a decrease of the material refractive index compared with a material whose properties would follow the additive laws. Those results confirm the existence of interactions between the PDMS and polyAcRf6 networks within such IPNs, already evidenced in the previous characterizations.

The hydrophobic character of a polymeric material can be estimated from contact angle measurements of a water drop deposited on its surface, the values of the contact angle depending on the chemical composition of the surface. Fluorinated polymers having good hydrophobic and oleophobic properties and silicones being hydrophobic as well, the contact angles measured on PDMS/polyAcRf6 IPNs should be larger than 90°. The association of two networks in an IPN architecture can lead to a material, the properties of which correspond to a value in between those of the two single partner networks.

The water contact angle measured on the PDMS single network surface is equal to  $\theta = 114^\circ$ . This value is higher than that reported in the literature for linear PDMS ( $\theta = 108^\circ$ ) [23]. This increase observed with the network could arise from the cross-linking step, which hinders the main chain movements normally occurring in the linear polymer and bringing a higher density of the hydrophobic material towards the surface. Similarly the cross-linking process also induces an increase in the water contact angle measured on fluorinated network compared with the fluorinated linear polymer. Indeed,  $\theta$  measured on the polyAcRf6 single network is equal to 117°, whereas the value reported for the linear polyAcRf6 is  $\theta = 113^\circ$  [24].

The contact angle of water drop deposited on PDMS/polyAcRf6 IPN surface has been measured on materials with various AcRf6 weight proportions (Fig. 6). Remarkably, the combination of the fluorinated and PDMS networks into an IPN architecture leads to a linear increase of the contact angle from 114° to 123° from single PDMS network to PDMS/polyAcRf6 (25/75) IPN, respectively. For AcRf6 contents higher than 75 wt%, the contact angle sharply decreases down to 117°, which is equal to the one measured on the polyAcRf6 single network surface. Thus the contact angle is maximum for the PDMS/polyAcRf6 (25/75) IPN and contrary to what is generally observed on copolymer surfaces [25], the contact angle does not vary monotonously with the AcRf6 weight proportion. Moreover, the contact angle measured on IPN surface is higher than the angle calculated from the linear combination

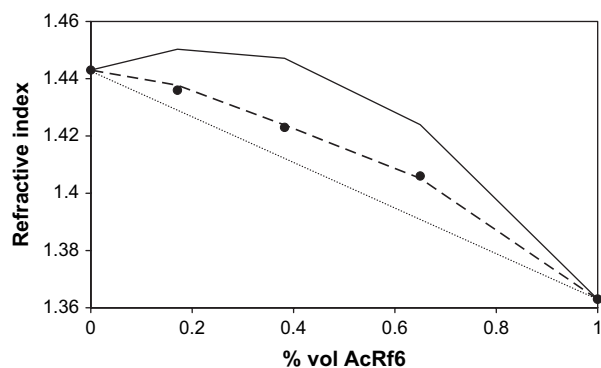


Fig. 5. Refractive index of PDMS/polyAcRf6 IPNs vs AcRf6 weight proportion calculated from the Lorentz–Lorentz equation using (dotted line) the IPN measured density and (black straight line) the additive law of the single network densities.

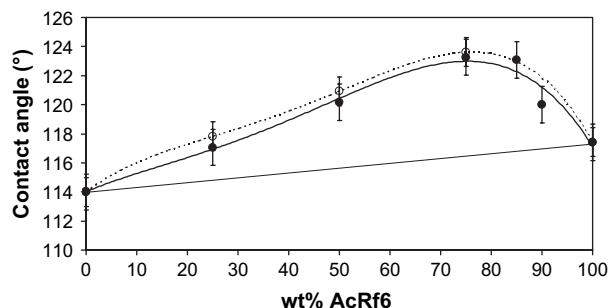


Fig. 6. Water contact angles of the surface of PDMS/polyAcRf6 IPNs vs AcRf6 weight proportion measured on IPNs before (●) and after (○) Soxhlet extraction with F113 for 48 h.

of the values measured on single network surface. Thus a true synergy of the surface properties is highlighted here.

In order to check that this phenomenon is intrinsic to the material and is not caused for example by the migration of unreacted and thus uncross-linked starting materials towards the surface, contact angles have been measured on the surface of the same IPNs before and after extraction in a Soxhlet extractor for 48 h with F113 (solvent of polyAcRf6). The results are reported in Fig. 6. Contact angles remain unchanged after this treatment, i.e. the observed phenomenon is specific to those IPNs.

Similar results of the non-linear variation of contact angle vs AcRf6 amount have been obtained with PDMS/polyAcRf6 IPNs in which the cross-linking density of the AcRf6 network is varied (EGDMA amounts from 3 to 10% by weight with respect to AcRf6) [22]. This modification hardly affects the values of contact angles measured on different IPN surfaces. In all cases, the largest contact angle is obtained for the AcRf6 75 wt% composition. Hare et al. [26] have shown that the low surface energy of fluorinated compounds and therefore the high contact angle values measured with water are due to the surface concentration of  $\text{CF}_3$  groups. The above IPN density measurements have shown that repulsive interactions are established in IPNs between PDMS and polyAcRf6 networks, resulting in a volume expansion of the material. During the IPN synthesis, the fluorinated grafts probably reorganize so as to minimize those repulsions and can in particular concentrate at the surface. Of course this repulsion phenomenon does not occur in the single fluorinated network. Thus the surface concentration of the fluorinated grafts could as a result be higher in the IPNs than in the single network. For weight proportions ranging between 75 and 85 wt%, the highest surface concentration in  $\text{CF}_3$  groups is reached. For proportions higher than 85 wt%, the fluorinated grafts are in a mainly fluorinated environment. In this case, the repulsion phenomenon decreases, the surface concentration of fluorinated grafts too, and the contact angle values accordingly.

Further characterization studies on the different IPN surfaces (XPS measurements) are in progress and the first measurements seem to confirm the results reported in this paper.

#### 4. Conclusion

An alternative leading to the elaboration of materials keeping only the advantageous characteristics of fluorinated polysiloxane single networks is to combine into interpenetrating polymer network (IPN) architectures, a polysiloxane on one hand and a fluorinated polymer on the other hand. All IPNs presented here have been synthesized according to an *in situ* strategy. Under the described experimental conditions, the fluorinated network is first formed which is the necessary condition in order to obtain a transparent material. The IPN mechanical relaxations studied by DMTA measurements are very broad and give no precise indications on the interpenetration degree of the networks in the IPN architecture. However, all IPNs exhibit only one glass transition, the position of which depends on the IPN composition. Moreover, PDMS/polyAcRf6 IPNs possess densities lower than those predicted by additive volume law. A volume expansion is observed on the synthesized IPN, probably due to the presence of repulsion forces developed between the networks. It was shown that this volume expansion has a direct influence on the refractive indices. Finally, the water contact angles measured on IPN surfaces do not vary linearly with the AcRf6 weight proportion. The values of these angles are higher than those calculated by linear combinations of angles measured on single network surfaces. Thus an interesting synergy of the surface properties is highlighted here.

Complementary surface studies on different IPNs by AFM and XPS will be presented in a forthcoming paper dealing with the surface properties of a series of IPNs combining the same AcRf6 network with different thermoplastic polymer networks.

#### References

- [1] Choi YS, Jun MS, Noh CS, Yang OB. Patent KR 2003043535, 2003.
- [2] Berglin M, Johnston E, Wynne K, Gatenholm P. ACS Symp Series 2001;787:96–111.
- [3] Guizard C, Boutevin B, Guida F, Ratsimihety A, Amblard P, Lasserre J-C, et al. Sep Purif Technol 2001;22–23:23–30.
- [4] Mignani G, Olier P, Priou C. Patent WO 2000000559, 2000.
- [5] Rash DM, Fiedler LD. Patent U.S. 4,898,903, 1990.
- [6] Fuduka K, Yamaguchi H, Arai M. Patent EP 1081192, 2001.
- [7] Sperling LH, Mishra V. The current status of interpenetrating polymer networks. In: Kim SC, Sperling LH, editors. IPNs around the world: science and engineering. New York: Wiley; 1997. p. 1–25.
- [8] Sperling LH. In: Klempner D, Sperling LH, Utracki LA, editors. Interpenetrating polymer networks. Advances in Chemistry Series 239. Washington, DC: American Chemical Society; 1994. p. 3–38.
- [9] Ni H, Aaserud DJ, Simonsick Jr WJ, Soucek MD. Polymer 1999;41: 57–71.
- [10] Mélas M. Ph.D. thesis, Montpellier II University, Montpellier; 1995.
- [11] Van Krevelen DW. Properties of polymers: their correlation with chemical structure; their numerical estimation and prediction from additive group contributions. completely revised. 3rd ed. Amsterdam: Elsevier; 1997.
- [12] Brandrup J, Immergut EH, Grulke EA. Polymer handbook. 4th ed. New York: Wiley; 1999.
- [13] Clarson SJ, Mark JE, Dodgson K. Polym Commun 1988;29:208–12.
- [14] Stansbury JW, Dickens SH. Dent Mater 2001;17:71–9.
- [15] Fichet O, Vidal F, Laskar J, Teyssié D. Polymer 2005;46:37–47.



- [16] Fontanille M, Gnanou Y. *Chimie et physico-chimie des polymères*. Paris: Dunod; 2002. p. 244.
- [17] Sophiea D, Klemperer D, Sendjarevic V, Suthar B, Frisch KC. In: Klemperer D, Sperling LH, Utracki LA, editors. *Interpenetrating polymer networks*. Advances in Chemistry Series 239. Washington, DC: American Chemical Society; 1994. p. 39–76.
- [18] Lu Y, Zhang L. *Polymer* 2002;43:3979–86.
- [19] Ben Khalifa R. Ph.D. thesis, Paris VI University, Paris; 1994.
- [20] Dubuisson A, Fontanille M, Zaoui A. *Rheol Acta* 1981;20:463–70.
- [21] Athawale VD, Pillay PS. *React Funct Polym* 2001;50:1–8.
- [22] Darras V. Ph.D. thesis, Paris XII, Créteil University; 2005.
- [23] Owen MJ. Surface properties and applications. In: Jones RG, Ando W, Chojnowski, editors. *Silicon-containing polymers*. Kluwer Academic Publishers; 2000. p. 213–32.
- [24] Corpart JM, Girault S, Juhue D. *Langmuir* 2001;17:7237–44.
- [25] Van de Grampel R, Van Geldrop J, Laven J, Van der Linde R. *J Appl Polym Sci* 2001;79:159–65.
- [26] Hare EF, Shafrin EG, Zisman WA. *J Phys Chem* 1954;58:236–9.